

Piezoelectric Bimorph Actuator with Integrated Strain Sensing Electrodes

Sepehr Zarif Mansour, Rudolf J. Seethaler
The University of British Columbia
Kelowna, Canada
sepehr.zmansour@alumni.ubc.ca

Yik R. Teo, Yuen K. Yong, Andrew J. Fleming
Precision Mechatronics Lab
The University of Newcastle
Callaghan, Australia

Abstract—This article describes a new method for estimating the tip displacement of piezoelectric benders. Two resistive strain gauges are fabricated within the top and bottom electrodes using an acid etching process. These strain gauges are employed in a half bridge electrical configuration to measure the surface resistance change, and estimate the tip displacement. Experimental validation shows a 1.1 % maximum difference between the strain sensor and a laser triangulation sensor.

I. INTRODUCTION

Piezoelectric actuators are used in a wide range of positioning applications such as micro-manipulating [1], vibration control [2], and Atomic Force Microscopy [3]. The most commonly used piezoelectric actuators in industrial applications are benders [4].

Bimorph benders consist of two piezoelectric plates that are bonded together. In order to provide reinforcement, a third elastic plate is sandwiched between the piezoelectric plates. In the cantilever configuration, an electric field is applied so that one plate expands while the other one contracts, which develops a net force and displacement at the tip.

Control of the tip displacement is a challenging task due to the lightly damped resonance and hysteresis [5], [6]. In a feedback control system, the tip displacement can be measured using an external displacement sensor. The displacement can also be estimated by bonding a strain gauge to the actuator surface, which is attractive due to the small form factor and low cost. The use of strain gauges as displacement sensors is commonly used for controlling piezoelectric stack actuators [7].

This article describes a new method for measuring the tip displacement of piezoelectric benders by integrating strain sensors into the top and bottom electrodes. The surface strain is shown to be directly proportional to the tip displacement. The strain gauges are implemented in a half bridge configuration which requires a bipolar amplifier circuit and avoids the need for an instrumentation amplifier.

In the remainder of the article, the experimental setup is described in Section II, an electromechanical model is derived in Section III, experimental results are presented in Section IV, and conclusions are discussed in Section V.

II. EXPERIMENTAL SETUP

The piezoelectric bimorph actuator is a Y-poled T220-A4-503Y from Piezo Systems. The dimensions are $63.5 \times 31.8 \times$

0.51 mm. It has a free displacement of ± 1 mm and a blocked force of ± 0.35 N. The internal construction is illustrated in Fig. 1. The layers include a 0.1 mm thick brass reinforcement layer shown in orange, two 0.2 mm thick piezoelectric plates shown in yellow, and two 5 μm layers of Nickel electrodes shown in blue.

Fig. 1(a) illustrates the process used to create the integrated strain gauge. First, a 0.1 mm thick resin mask is printed on the electrode using a Form 2 Desktop 3D printer with 5 μm resolution. Then 30% nitric acid is used to etch the electrode area not covered by the mask. The desired electrode feature is an electrically isolated U-shaped strain gauge with an effective length of 40 mm and a width of 1 mm. This process is carried out on both top and bottom electrodes.

Fig. 1(b) describes the experimental setup. The bender is cantilevered with a free length of 57 mm. It is driven in a parallel electrical configuration where the middle brass layer is grounded and ± 90 V signal u is applied to the external electrodes by a PiezoDrive PD200 amplifier. The reference sensor is a Di-Soric LAT61 laser displacement sensor.

The strain gauges are excited in a half bridge configuration by applying a DC voltage to the top V_t and bottom strain gauge V_b . By tuning either V_t or V_b , the voltage at the center of the half bridge V_c can be set to zero. V_c is then amplified by a gain K , which provides a voltage which is proportional to the tip displacement. The sensitivity K_s is found experimentally

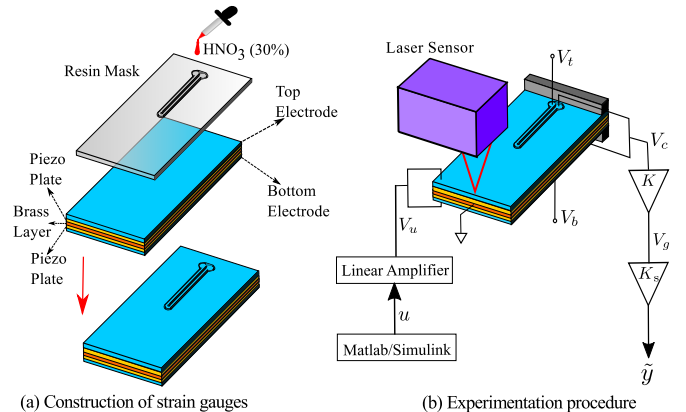


Fig. 1. Experimental setup.

using the reference sensor. The estimated tip displacement is \tilde{y} in Fig. 1(b).

III. ELECTROMECHANICAL MODEL OF THE PIEZOELECTRIC BENDER

This work uses the basic principles as standard resistive strain gauges. That is, the electrical resistance change is related to the surface strain. In benders, surface strain is also related to the tip displacement. Hence, the tip displacement of a bender can be estimated by measuring its surface resistance change. Section A derives a proportionality between surface strain and tip displacement. Section B relates the resistance change to tip displacement.

A. Tip Displacement and Surface Strain Relationship in Benders

In this study, Euler-Bernoulli beam theory is used. Tip displacement is considered to be relatively small, no external forces are exerted on the bender, and the driving voltage V_u is assumed to be effective across the thickness h of each piezoelectric plate. In Fig. 2, l_s is the nominal length of the strain gauges and t is a 0.5 mm gap which separates them from the high-voltage electrode. Using the constitutive equation for the inverse piezoelectric effect [8], the stress σ in each piezoelectric plate is,

$$\sigma = d_{31}E \frac{V_u}{h} + E\epsilon(x), \quad (1)$$

where, d_{31} is the piezoelectric constant, E is the Young's modulus, and $\epsilon(x)$ is the strain along the neutral axis. For relatively small tip displacements, $\epsilon(x)$ in (1) is replaced with $\epsilon(x) = -y \frac{d^2y}{dx^2}$, where y is the vertical distance from the neutral axis. The moment due to the external forces $M(x)$ can then be calculated by taking the integral of σy , over the cross-sectional area of the bender [4], that is

$$M(x) = d_{31}EV_u w \frac{h}{2} - EI \frac{d^2y}{dx^2}. \quad (2)$$

In (2), I is the moment of inertia and w is the width of the bender. Given the fact that external forces are assumed to be absent, $M(x) = 0$, which simplifies (2) to,

$$\frac{d^2y}{dx^2} = d_{31}V_u w \frac{h}{2I}, \quad (3)$$

which indicates that the bender is experiencing a pure bending due to the applied driving voltage. Solving for y , at $x = L$, the tip displacement is,

$$y_{\text{tip}} = \frac{d_{31}V_u w h L^2}{2I}. \quad (4)$$

Using (3), the average surface strain $\epsilon_{\text{ave,t}}$ along the top sensor length l_s is

$$\epsilon_{\text{ave,t}} = \frac{1}{l_s} \int_t^{l_s+t} \epsilon(x) = \frac{-d_{31}V_u w h^2}{2I} \quad (5)$$

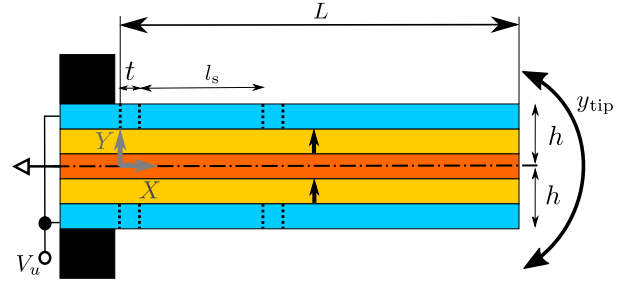


Fig. 2. Electromechanical model of the bender.

Comparing (4) with (5), the tip displacement y_{tip} and the average strain $\epsilon_{\text{ave,t}}$ are proportional. The proportionality is

$$\frac{y_{\text{tip}}}{\epsilon_{\text{ave,t}}} = -\frac{L^2}{2h}. \quad (6)$$

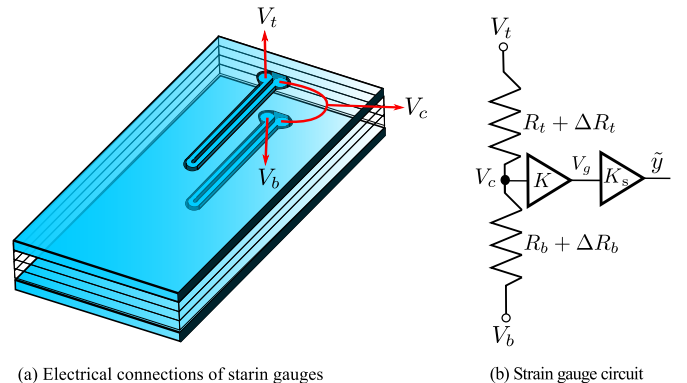
B. Surface Resistance change Measurement

Fig. 3(a) illustrates the electrical connection of the integrated strain gauges. A conditioning circuit provides the top and bottom strain gauges with constant DC voltages of V_t and V_b . The equivalent circuit is shown in Fig. 3(b) where the nominal resistance of the top and bottom gauges is R_t and R_b respectively. When the bender moves, the top and bottom gauges experience a change in resistance ΔR_t and ΔR_b .

Assuming that the top and bottom sensors experience identical strain, $\epsilon_{\text{ave}} = \epsilon_{\text{ave,t}} = -\epsilon_{\text{ave,b}}$,

$$\epsilon_{\text{ave}} \propto \frac{\Delta R_t}{R_t} \propto \frac{\Delta R_b}{R_b}. \quad (7)$$

Using (6) and (7), the tip displacement can be estimated by measuring the resistance change, which is proportional to V_c . The excitation voltages V_t and V_b are tuned so that the nominal value of V_c is zero. When this is achieved, $\left(\frac{V_t}{V_b} = -\frac{R_t}{R_b}\right)$.



(a) Electrical connections of strain gauges

(b) Strain gauge circuit

Fig. 3. The electrical connection of the strain gauges (a) and the equivalent circuit (b).

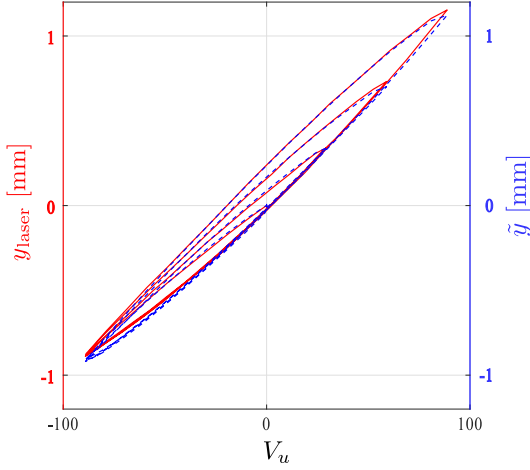


Fig. 4. Hysteresis measured by the reference and strain sensors.

In the presence of strain, assuming that the strain gauges are identical ($R_t = R_b$), the voltage V_c is

$$V_c \propto \frac{\Delta R_t}{R_t} \propto \frac{\Delta R_b}{R_b}. \quad (8)$$

Using a gain of K , this voltage is amplified to $V_g = KV_c$. Equations (6-8) give,

$$V_g \propto y_{tip}. \quad (9)$$

The proportionality (9), experimentally derived in the next section. The estimated displacement \tilde{y} is then given by

$$\tilde{y} = K_s V_g. \quad (10)$$

IV. EXPERIMENTAL RESULTS

The proposed method is demonstrated by applying a triangular driving voltage V_u to the actuator at 33%, 67%, and 100% of the full-scale voltage (± 90 V). The resulting tip displacement measured by both the reference and strain sensor

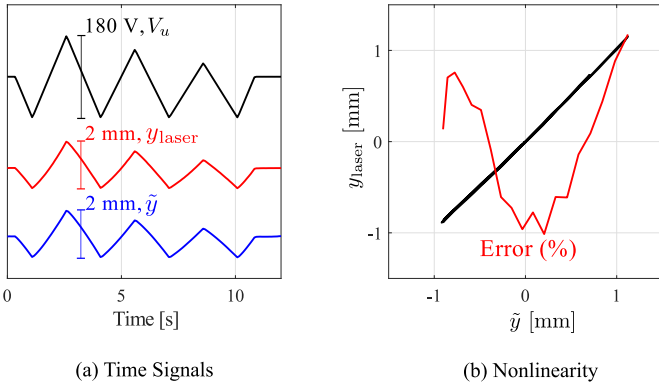


Fig. 5. The recorded time signals (a) and difference between the reference and proposed sensor (b). In (a), the peak-to-peak values are provided for the actuator voltage V_u , the reference sensor y_{laser} , and strain sensor \tilde{y} .

are plotted in Fig. 4. The piezoelectric hysteresis can be clearly observed in both signals.

Time signals are plotted in Fig. 5(a), where a close agreement between the reference and strain sensor can be observed. In Fig. 5(b), the output of the reference and strain sensor are plotted against each other. The difference between the two sensors is calculated as a percentage of full range, based on a least-squares fit for the sensitivity and offset. The maximum difference is 1.1 % of the full-range displacement. A polynomial calibration function could be used to significantly reduce the residual error.

V. CONCLUSION

The article presents a new method for estimating the tip displacement of piezoelectric benders by integrating resistive strain gauges into the top and bottom electrodes. The change in surface resistance is shown to be proportional to the tip displacement in the absence of external forces. The strain gauges are employed in a half bridge configuration to measure the resistance change and tip displacement.

The presented method is experimentally compared to a reference sensor. The maximum difference between the two sensor outputs was 1.1% of full range. Future work will consider external forces and optimization of the sensor geometry.

ACKNOWLEDGMENT

The authors would like to thank Mr. Ben Routley for his assistance developing the etching process.

REFERENCES

- [1] A. M. El-Sayed, A. Abo-Ismael, M. T. El-Melegy, N. A. Hamzaid, and N. A. A. Osman, "Development of a micro-gripper using piezoelectric bimorphs," *Sensors*, vol. 13, no. 5, pp. 5826–5840, 2013.
- [2] A. J. Fleming, "Nanopositioning system with force feedback for high-performance tracking and vibration control," *IEEE/ASME Transactions on Mechatronics*, vol. 15, no. 3, pp. 433–447, 2010.
- [3] Y. K. Yong and A. J. Fleming, "High-speed vertical positioning stage with integrated dual-sensor arrangement," *Sensors and Actuators A: Physical*, vol. 248, pp. 184–192, 2016.
- [4] S. A. Rios and A. J. Fleming, "A new electrical configuration for improving the range of piezoelectric bimorph benders," *Sensors and Actuators A: Physical*, vol. 224, pp. 106–110, 2015.
- [5] —, "Design of a charge drive for reducing hysteresis in a piezoelectric bimorph actuator," *IEEE/ASME Transactions on Mechatronics*, vol. 21, no. 1, pp. 51–54, 2016.
- [6] M. N. Islam and R. J. Seethaler, "Sensorless position control for piezoelectric actuators using a hybrid position observer," *IEEE/ASME Transactions On Mechatronics*, vol. 19, no. 2, pp. 667–675, 2014.
- [7] A. J. Fleming and K. K. Leang, "Integrated strain and force feedback for high-performance control of piezoelectric actuators," *Sensors and Actuators A: Physical*, vol. 161, no. 1, pp. 256–265, 2010.
- [8] D. Hall, "Review nonlinearity in piezoelectric ceramics," *Journal of materials science*, vol. 36, no. 19, pp. 4575–4601, 2001.